

# Superheavy Nuclei: Relativistic Mean Field Outlook.

A. V. Afanasjev <sup>\*</sup>

*Department of Physics, University of Notre Dame, Notre Dame, Indiana 46556, USA and  
Department of Physics and Astronomy, Mississippi State University, MS 39762, USA*

(Dated: October 8, 2018)

The analysis of quasiparticle spectra in heaviest  $A \sim 250$  nuclei with spectroscopic data provides an additional constraint for the choice of effective interaction for the description of superheavy nuclei. It strongly suggest that only the parametrizations of the relativistic mean field Lagrangian which predict  $Z = 120$  and  $N = 172$  as shell closures are reliable for superheavy nuclei. The influence of the central depression in the density distribution of spherical superheavy nuclei on the shell structure is studied. Large central depression produces large shell gaps at  $Z = 120$  and  $N = 172$ . The shell gaps at  $Z = 126$  and  $N = 184$  are favored by a flat density distribution in the central part of nucleus. It is shown that approximate particle number projection (PNP) by means of the Lipkin-Nogami method removes pairing collapse seen at these gaps in the calculations without PNP.

PACS numbers: 21.60.Cs, 21.60.Jz, 27.90.+b, 21.10.Pc, 21.10.Ft, 21.10.Gv

The possible existence of shell-stabilized superheavy nuclei, predicted with realistic nuclear potentials and the macroscopic-microscopic (MM) method (see references quoted in Ref. [1]), has been a driving force behind experimental and theoretical efforts to investigate superheavy nuclei. These investigations pose a number of challenges. The recent discovery of elements with  $Z = 115$  [2] and  $Z = 116$  [3] clearly shows great progress on the experimental side, but also indicates difficulties in the investigation of nuclei with low production cross sections and analyses based on few events.

The theoretical challenges are also considerable since different theoretical methods predict different spherical shell closures such as  $Z = 114, 120, 126$  for protons and  $N = 172, 184$  for neutrons [4]. The largest variation in the predictions of shell closures appear in the self-consistent calculations based either on non-relativistic (Skyrme and Gogny [5]) or relativistic (relativistic mean field [RMF] [6]) density functionals. Unfortunately, the properties of known superheavy nuclei in their ground states do not allow to discriminate between these predictions [7]. This is due to the fact that known region of superheavy elements is dominated by  $\alpha$  decay, but  $\alpha$ -decays occur between neighbouring nuclei and their half-lives are only insignificantly modified by shells effects [8].

The part of these variations is definitely related to the fact that there is a large variety of the parametrizations for self-consistent models, but for many of them even the reliability of describing conventional nuclei is poorly known. In addition, self-consistent calculations have been confronted with experiment to a lesser degree and for a smaller number of physical observables (mainly binding energies and quantities related to their derivatives) as compared with MM method. In particular, little attention has been paid to single-particle degrees of freedom within the self-consistent models. However,

the accuracy of predictions of spherical shell closures depends sensitively on the accuracy of describing the single-particle energies, which becomes especially important for superheavy nuclei where the level density is high.

Sect. I shows how the study of quasiparticle states in odd-mass nuclei of the  $A \sim 250$  region within the cranked relativistic Hartree-Bogoliubov (CRHB) theory [9] constrains the choice of the RMF parametrization for the study of superheavy nuclei. The implications of such investigation for these nuclei are also discussed (Sect. I). The influence of central depression in density distribution on the shell structure of spherical superheavy nuclei is discussed in Sect. II. The importance of particle number projection for the description of pairing properties of spherical superheavy nuclei is shown in Sect. III. Finally, Sect. IV summarizes main conclusions.

## I. THE $A \sim 250$ MASS REGION TEST

The investigation of the single-particle states in the odd-mass deformed nuclei of the  $A \sim 250$  mass region (the heaviest nuclei for which detailed spectroscopic data are available) shed additional light on the reliability of the predictions of RMF theory on the energies of spherical subshells responsible for 'magic' numbers in superheavy nuclei. This is because several deformed single-particle states experimentally observed in odd nuclei of the  $A \sim 250$  region originate from these subshells (see Table 3 in Ref. [1]).

The comparison between experimental and mean field single-particle states is less ambiguous in deformed nuclei as compared with spherical ones [10, 11] at least at low excitation energies, where vibrational admixtures to the wave function are small. This is a result of the surface vibrations being less collective in deformed nuclei than in spherical ones since they are more fragmented [10, 12]. As a consequence, the corrections to the energies of quasiparticle states in odd nuclei due to particle-vibration coupling are less state-dependent in deformed

---

<sup>\*</sup>Email address: aafanasj@nd.edu

nuclei.

A proper description of odd nuclei implies the loss of the time-reversal symmetry of the mean-field, which is broken by the unpaired nucleon. The BCS approximation has to be replaced by the Hartree-(Fock-)Bogoliubov method, with time-odd mean fields taken into account. The breaking of time-reversal symmetry leads to the loss of the double degeneracy (Kramer's degeneracy) of the quasiparticle states. This requires the use of the signature or simplex basis in numerical calculations, thus doubling the computing task. Furthermore, the breaking of the time-reversal symmetry leads to nucleonic currents, which cause *nuclear magnetism* [13]. The CRHB(+LN) theory [9, 14] takes all these effects into account.

First ever fully self-consistent description of quasiparticle states in the framework of the RMF theory was presented in Ref. [1] on the example of  $^{249,251}\text{Cf}$  and  $^{249}\text{Bk}$  nuclei. Fig. 1 shows the CRHB results for  $^{251}\text{Cf}$ . Although the same set of quasiparticle states as in experiment appears, the calculated spectra are less dense. This is related to the effective mass (Lorentz mass in the notation of Ref. [15]) of the nucleons at the Fermi surface  $m^*(k_F)/m$ . While the experimental density of the quasiparticle levels corresponds to  $m^*(k_F)/m$  close to one, the low effective mass  $m^*(k_F)/m \approx 0.66$  of the RMF theory [16] leads to a stretching of the energy scale. It has been demonstrated for spherical nuclei that the particle-vibration coupling brings the average level density in closer agreement with experiment [10]. Similar effect is expected in deformed nuclei.

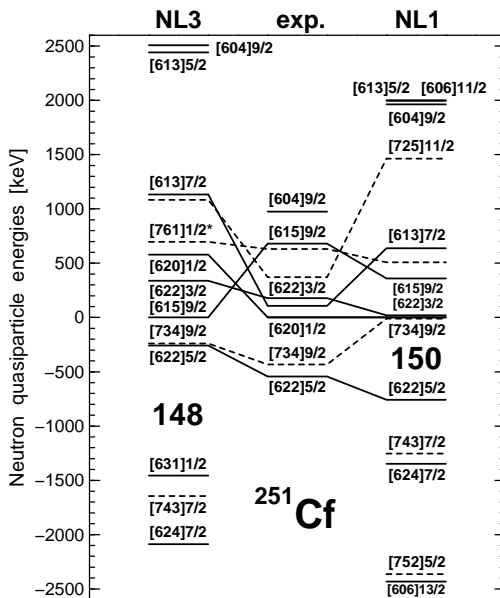


FIG. 1: Experimental and theoretical quasiparticle energies of neutron states in  $^{251}\text{Cf}$ . Positive and negative energies are used for particle and hole states, respectively. Solid and dashed lines are used for positive and negative parity states, respectively. The symbols 'NL3' and 'NL1' indicate the RMF parametrization. From Ref. [1]

The calculated energies of a number of states are rather close to experiment. On the other hand, the energies of some states and their relative positions deviate substantially from experiment. For example, only NL1 gives the correct ground state  $\nu[620]1/2$  in  $^{251}\text{Cf}$ , whereas NL3 gives the  $\nu[615]9/2$  (Fig. 1). Detailed analysis shows that the discrepancies between experiment and calculations can be traced back to energies of spherical subshells from which deformed states emerge. This allows us to define 'empirical shifts' to the energies of spherical subshells (see Ref. [1] for details), which, if incorporated, will correct the discrepancies between calculations and experiment seen for deformed quasiparticle states. These 'empirical shifts' are shown in Fig. 2 as the energy difference between self-consistent and corrected energies of specific subshells.

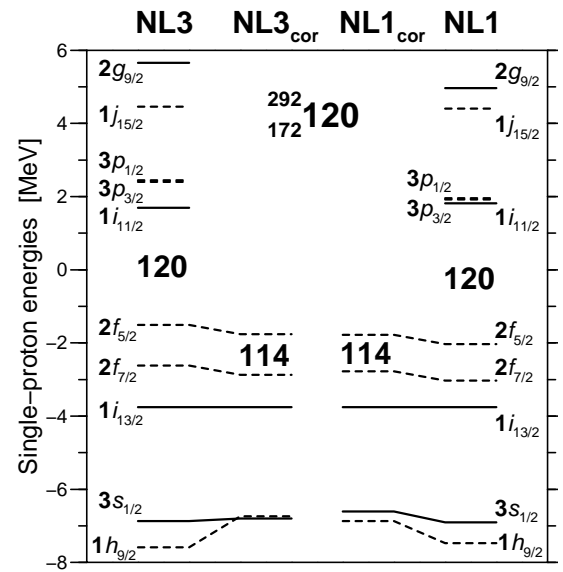


FIG. 2: Proton single-particle states in a  $^{292}_{172}\text{Bk}$  nucleus. Columns 'NL3' and 'NL1' show the states obtained in the RMF calculations at spherical shape with the indicated parametrizations. The energy of the  $1i_{13/2}$  state in the NL1 parametrization is set to be equal to that in NL3, which means that the energies of all states in NL1 (last column) are increased by 0.78 MeV. The columns 'NL3<sub>cor</sub>' and 'NL1<sub>cor</sub>' show how the spectra are modified if empirical shifts were introduced based on discrepancies between calculations and experiment for quasiparticle spectra in deformed  $^{249}\text{Bk}$ . Solid and dashed lines are used for positive and negative parity states. Spherical gaps at  $Z = 114$  and  $Z = 120$  are indicated. From Ref. [1]

In the NL1 and NL3 parametrizations, the energies of the spherical subshells, from which the deformed states in the vicinity of the Fermi level of the  $A \sim 250$  nuclei emerge, are described with an accuracy better than 0.5 MeV for most of the subshells (see Fig. 2 in the present manuscript and Fig. 28 in Ref. [1]: 'empirical shifts', i.e. corrections, for single-particle energies are indicated in both figures). The discrepancies (in the range

of  $0.6 - 1.0$  MeV) are larger for the  $\pi 1h_{9/2}$  (NL3, NL1),  $\nu 1i_{11/2}$  (NL3),  $\nu 1j_{15/2}$  (NL1) and  $\nu 2g_{9/2}$  (NL3) spherical subshells. Considering that the RMF parametrizations were fitted only to bulk properties of spherical nuclei this level of agreement is good.

In contrast, the accuracy of the description of single-particle states is unsatisfactory in the NLSH and NL-RA1 parametrizations, where 'empirical shifts' to the energies of some spherical subshells are much larger than in NL1 and NL3. NL-SH and NL-RA1 are the only RMF sets indicating  $Z = 114$  as a magic proton number [17, 18]. In the light of present results, these parametrizations should be considered as unreliable.

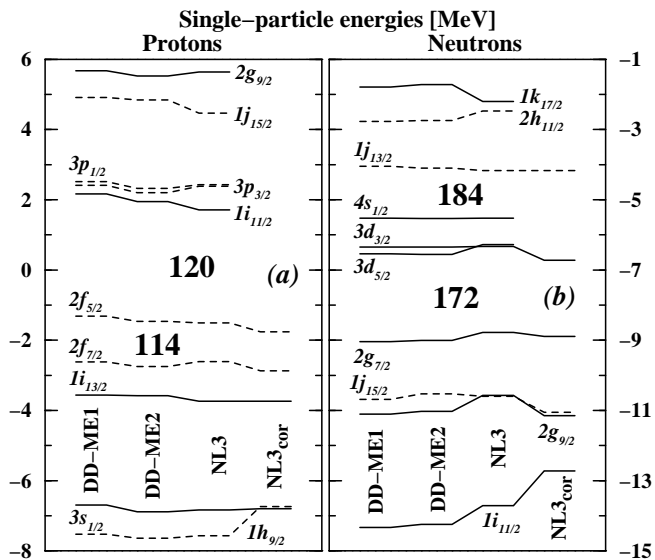


FIG. 3: Single-particle spectra of the  $^{292}120$  nucleus. Columns 'DD-ME2', 'DD-ME1' and 'NL3' show the states obtained in the RMF calculations at spherical shape with the indicated parametrizations. The column 'NL3<sub>cor</sub>' shows the spectra modified by empirical shifts. Solid and dashed lines are used for positive and negative parity states.

It is interesting to compare the results obtained through non-linear parametrizations of the RMF Lagrangian (NL1 and NL3) with the ones based on the parametrizations which include an explicit density dependence of the meson-nucleon couplings (DD-ME1 [19] and DD-ME2 [20]). The latter parametrizations provide an improved description of asymmetric nuclear matter, nucleon matter, and nuclei far from stability [20]. However, the single-particle spectra of the  $^{292}120$  nucleus obtained with DD-ME1 and DD-ME2 are similar to the ones seen in NL3 (Fig. 3). When compared with the NL3 spectra corrected for 'empirical shifts' (columns NL3<sub>cor</sub> in Fig. 3, one can see that the DD-ME2 and DD-ME1 parametrizations do not remove the problems of the description of proton  $\pi 1h_{9/2}$  state (Fig. 3a) and provide worse description of neutron  $\nu 1i_{11/2}$  state as compared with NL3 set (see Ref. [1] for more detailed discussion of these states).

The measured and calculated energies of the single-particle states at normal deformation provide constraints on the spherical shell gaps of superheavy nuclei. Such analysis restricts the choice of the RMF parametrizations only to those which predict  $Z = 120$  and  $N = 172$  as shell closures in superheavy nuclei [1]. In general, since the accuracy of the description of the  $\nu 4s_{1/2}$  state is unknown, we cannot also exclude the existence of the  $N = 184$  gap [1]. Similar analysis to Ref. [1] in non-relativistic models would restrict the choice of effective forces. However, it is already clear that the SkI4 Skyrme force which predicts  $Z = 114$  shell gap can be ruled out since it provides poor description of the spin-orbit splittings [16]. Thus, one can conclude that non-relativistic theories suggest the existence of shell gaps (not necessary doubly shell closures) at  $Z = 120, 126$  and  $N = 172, 184$  (see Ref. [21] and references quoted therein). The role of self-consistency effects in the appearance of these shell gaps is discussed in the next section.

## II. SELF-CONSISTENCY EFFECTS IN SUPERHEAVY SPHERICAL NUCLEI

Self-consistent microscopic calculations find a central depression in the nuclear density distribution [16, 22], which generates a wine-bottle nucleonic potential. The influence of this depression on the shell structure of spherical superheavy nuclei has been studied in Ref. [21] within the RMF theory without pairing.

The underlying microscopic mechanism for an appearance of this central density depression is illustrated in Fig. 4. The starting point of this consideration is the density distribution in  $^{208}\text{Pb}$ , which is nearly flat in central region of nucleus. Its charge distribution is well described by the RMF theory [23, 24]. It is general feature of all nuclear structure models that on going from  $^{208}\text{Pb}$  to spherical superheavy nuclei in the region around  $Z = 120$  and  $N = 172$ , the ground state configurations are built first by the occupation of the group of high- $j$  subshells (neutron  $\nu 1i_{11/2}$ ,  $\nu 1j_{15/2}$ , and  $\nu 2g_{9/2}$  and proton  $\pi 1i_{13/2}$  and  $\pi 1h_{9/2}$ ) and then by the occupation of the group of medium- $j$  subshells (neutron  $\nu 2g_{9/2}$  and proton  $2f_{7/2}$  and  $2f_{5/2}$ ), see Fig. 4. The high- $j$  subshells are localized mostly near the surface, whereas the low- $j$  subshells have a more central localization. As a consequence of this grouping of high- $j$  and medium- $j$  subshells above  $^{208}\text{Pb}$ , the density is added mostly in the surface region which leads to the appearance of the central density depression in the nuclei around the  $Z = 120, N = 172$  system, see Fig. 4.

On the contrary, the group of low- $j$  subshells (neutron  $\nu 3d_{5/2}$ ,  $\nu 3d_{3/2}$  and  $\nu 4s_{1/2}$  and proton  $\pi 3p_{3/2}$  and  $\pi 3p_{1/2}$ ) is filled on going from the  $Z = 120, N = 172$  system to the  $Z = 126, N = 184$  system. Since filling up a low- $j$  group with nucleons increases the density near the center, the density distribution in the central part of nucleus is nearly flat in the latter system.

The magic gaps of the wine-bottle (the case of central depression in density distribution) and flat-bottom (the case of flat density distribution) nucleonic potentials are different. This is illustrated in Fig. 5, where starting from the ground state configuration of  $^{292}120_{172}$  nucleus, having a central depression (configuration 'g-s'), a flatter density distribution in the central part of nucleus is generated by exciting particles from high- $j$  subshells to low- $j$  subshells (configuration 'exc-s') [21]. While wine-bottle potential (conf. 'g-s') is characterized by the large  $Z = 120$  and  $N = 172$  large gaps, we see the appearance of the  $Z = 126$  proton gap and the shrinking of the  $Z = 120$  shell gap in the flat-bottom potential (conf. 'exc-s'). To a lesser extend, the  $N = 172$  neutron gap decreases and the  $N = 184$  gap increases in the latter potential.

Due to the isovector force, which tries to keep the neutron and proton density profiles alike, there is a mutual enhancement of the  $Z = 120$  and  $N = 172$  gaps, both being favored by the wine-bottle potential, and of the  $Z = 126$  and  $N = 184$  gaps, both favored by the flat bottom potential. For the same reason the gaps are smaller for the combination  $Z = 126$  and  $N = 172$ , and the  $Z = 120$  gap does not develop for the  $N = 184$  systems. This behavior is not expected to depend much on the density functional chosen (see discussion in Ref. [21]).

Considering that  $Z = 120, 126$  and  $N = 172, 184$  are the particle numbers which appear as the candidates for 'magic' particle numbers in self-consistent theories, it is clear that the magnitude of the central depression in density distribution is an important factor in defining 'magic'

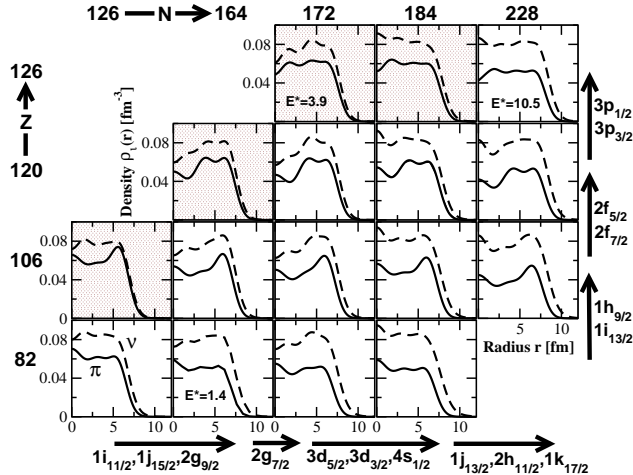


FIG. 4: The evolution of proton and neutron densities with the changes of proton and neutron numbers. Arrows indicate the group of single-particle subshells which become occupied with the change of the nucleon number. The figure is based on the results of spherical RMF calculations without pairing employing the NL3 [25] parametrization. The shaded background is used for nuclei located beyond the proton-drip line. If the indicated configuration is not lowest in energy, its excitation energy (in MeV) is given by  $E^*$ . From Ref. [21]

shell gaps in spherical superheavy nuclei. This magnitude is correlated with effective mass  $m^*/m$  of microscopic theory: more pronounced central depression develops for the density functionals with low effective mass [16]. This feature may be understood as follows [21]. In the surface region,  $m^*/m$  changes from low value ( $< 1$ ) in the interior to 1 in the exterior. Classically, nucleons with given kinetic energy are more likely to be found in regions with high effective mass than in the regions with low one because they travel with lower speed. This is reflected by the Thomas-Fermi expression for the nucleonic density  $\rho \propto [2m^*(\epsilon_F - V)]^{3/2}$ . The increase of the effective mass in the surface region favors the transfer of mass from the center there, which makes the above discussed polarization mechanism of the high- $j$  subshells more effective for functionals with low effective mass.

All experimentally known nuclei with  $Z \geq 100$  are expected to be deformed [26, 27]. The deformation leads to a more equal distribution of the single-particle states emerging from the high- $j$  and low- $j$  spherical subshells (see, for example, the Nilsson diagrams in Figs. 3-4 in Ref. [28]) than for spherical shape. Thus, the density profile of a deformed nucleus is relatively flat [21, 29], strongly resembling the one of phenomenological potentials. In addition, the density profile variations as a function of particle number are less drastic than in spherical nuclei. These features together with the fact that the

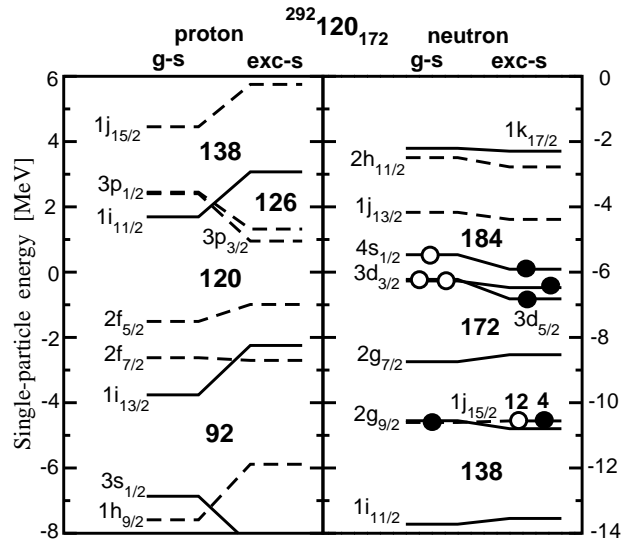


FIG. 5: Single-particle spectra of the ground state (indicated as 'g-s') and the excited (indicated as 'exc-s') configurations in the  $^{292}120_{172}$  system obtained in the RMF calculations with the NL3 force. Solid and dashed lines are used for positive and negative parity, respectively. Solid and open circles indicate the occupied and empty subshells, respectively. In the ground state, all subshells below  $Z = 120$  and  $N = 184$  are fully occupied. In the excited configuration, only 12 particles are excited from the subshell  $\nu 1j_{15/2}$ : 4 particles still reside in this subshell. The spherical shell gaps of interest are indicated. From Ref. [21]

single-particle energies of the deformed nuclei in heavy actinide region have been carefully fitted in the phenomenological potentials explains the success of the shell correction method [30, 31] in the description of known superheavy nuclei. However, this method neglects the self-consistent rearrangement of single-particle levels due to the appearance of a central depression in spherical superheavy nuclei. Thus the predictions of the magic numbers for superheavy nuclei within the shell correction method should be considered with caution.

### III. PAIRING CORRELATIONS IN SUPERHEAVY NUCLEI.

Almost all published self-consistent calculations for superheavy nuclei performed either in an approximate HF+BCS or full Hartree-Fock-Bogoliubov (HFB) frameworks show the collapse of pairing at large shell gaps in spherical superheavy nuclei (see, for example, Refs. [17, 32, 33]). Principal shortcoming of these calculations is the fact that neither the BCS nor the HFB wave functions are the eigenstates of particle number operator [1, 34]. The best way to deal with this problem would be to perform an exact particle number projection before the variation [34], but this is very time-consuming for realistic interactions. In this section, the importance of particle number projection on the properties of spherical superheavy nuclei is studied employing the CRHB theory [9] with and without approximate particle number projection by means of the Lipkin-Nogami (LN) method.

The CRHB(+LN) calculations are performed using the NL3 parametrization for the RMF Lagrangian and Gogny D1S force in the pairing channel. The scaling factors  $f$  of the Gogny D1S force are selected as follows:  $f = 1.0$  in the calculations without LN (CRHB) and  $f = 0.864$  in the calculations with LN (CRHB+LN). These scaling factors provide good description of the moments of inertia of rotational bands in the  $A \sim 250$  mass region [1].

Figs. 6a,b compare the calculated pairing energies  $E_{pairing} = -\frac{1}{2}Tr(\Delta\kappa)$  for  $Z = 120$  isotopes obtained in the CRHB and CRHB+LN calculations. The  $Z = 120$  gap is large in the vicinity of  $N = 172$  (see Sect. II) which leads to the collapse of proton pairing in the CRHB calculations (Fig. 6b). With increasing neutron number, the densities in the central part of nuclei become flatter (see Sect. II) leading to shrinking of the  $Z = 120$  gap. Because of that the proton pairing shows up at  $N = 182$  and increases in absolute magnitude with the increase of  $N$  (Fig. 6b). Because neutron  $N = 172$  and  $N = 184$  gaps are smaller than the  $Z = 120$  gap (Fig. 3), the pairing collapse in neutron subsystem is seen only at these neutron numbers (Fig. 6b). Similar collapse of pairing is seen at 'magic' shell closures in the CRHB calculations for the  $N = 172$  and  $N = 184$  isotones (not shown here). On the contrary, no pairing collapse is observed in the CRHB+LN calculations for these chains of nuclei (Figs.

6a,c). In addition, smaller variations of  $E_{pairing}$  as a function of particle number are seen in the CRHB+LN calculations as compared with the CRHB ones.

It was suggested in Ref. [33] to use the fact that the pairing energies vanish at closed shells as a fingerprint of the shell gaps. Present studies in the CRHB+LN framework do not support this suggestion. One should also note that the LN method maybe less reliable in the regime of weak pairing [35] typical for large shell gaps, so more detailed investigation of the pairing in spherical superheavy nuclei in the formalism with exact particle number projection is needed.

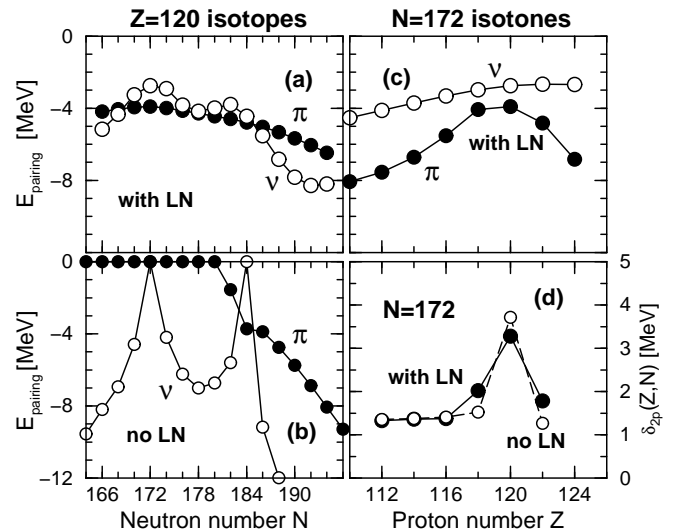


FIG. 6: Pairing energies  $E_{pairing}$  as a function of particle number obtained in the CRHB calculations with (panels (a) and (c)) and without (panel (b)) approximate particle number projection by means of the Lipkin-Nogami method for the  $Z = 120$  isotopes (panels (a) and (b)) and  $N = 172$  isotones (panel (c)). Panel (d) shows the  $\delta_{2n}(Z, N)$  quantity for the  $N = 172$  isotones obtained in the CRHB calculations with and without LN.

One of the observables used frequently in the search of shell gaps in superheavy nuclei is the  $\delta_{2n,(2p)}(N, Z)$  quantity (called sometimes as two-nucleon shell gap [see Ref. [1] for the discussion of this quantity]) which for the neutrons (and similarly for the protons) is defined as

$$\delta_{2n}(Z, N) = S_{2n}(Z, N) - S_{2n}(Z, N + 2)$$

This quantity is related to the derivative of the separation energy  $S_{2n}(Z, N)$ , and thus, it is a sensitive indicator of the localization of the shell gaps. As follows from the comparison of the CRHB and CRHB+LN calculations (Figs. 6c and d), the presence of pairing at shells gaps affects the  $\delta_{2n,(2p)}(N, Z)$  quantity in the following way: the peak in  $\delta_{2n,(2p)}(N, Z)$  becomes more smooth and broad and the magnitude of it decreases.

#### IV. CONCLUSION

The analysis of quasiparticle spectra in heaviest  $A \sim 250$  nuclei provides an additional constraint for the choice of effective interaction for the description of superheavy nuclei within specific model. Based on this analysis it was concluded that only parametrizations of the RMF Lagrangian predicting  $Z = 120$  and  $N = 184$  as shell closures provide reasonable description of the spectra of odd-mass nuclei. No support for the  $Z = 114$  shell gap has been established. One can restrict the predictions of self-consistent models (including non-relativistic ones) to shell gaps at  $Z = 120, 126$  and  $N = 172, 184$ . The investigation of self-consistency effects related to central depression in the density distribution finds important correlations between these gaps: large central depression produces large shell gaps at  $Z = 120$  and  $N = 172$ , while the shell gaps at  $Z = 126$  and  $N = 184$  are favored by a flat density distribution in the central part of nucleus. However, the magnitude of the central depression correlates with an effective mass of nucleon in specific model/parametrization. Unfortunately, there is no con-

sensus on what value an effective mass should have in self-consistent theories (see, for example, the discussion in Refs. [36]). Because of existing differences in effective mass of nucleon in different models/parametrizations (especially pronounced for Skyrme forces), the studies of quasiparticle spectra in deformed actinide nuclei may not provide sufficient constraint for localization of magic double shell closure (if any) in spherical superheavy nuclei. Approximate particle number projection (PNP) by means of the Lipkin-Nogami method removes pairing collapse seen at large shell gaps in spherical superheavy nuclei in the calculations without PNP. Since closed shell nuclei maybe in the regime of weak pairing, more detailed studies of the pairing properties of superheavy nuclei in the formalism with an exact particle number projection are needed.

#### Acknowledgements

This work was supported by the DOE grant DE-F05-96ER-40983. I would like to express my gratitude to S. Frauendorf, T. L. Khoo, G. Lalazissis, and I. Ahmad for their contributions into this project.

---

[1] A. V. Afanasjev, T. L. Khoo, S. Frauendorf, G. A. Lalazissis, and I. Ahmad, Phys. Rev. C **67**, 024309 (2003).

[2] Yu. Ts. Oganessian *et al*, Phys. Rev. C 69, 021601(R) (2004).

[3] Yu. Ts. Oganessian *et al*, Phys. Rev. C 63, 011301(R) (2000).

[4] P.-G. Reinhard, M. Bender, and J. A. Maruhn, Comments Mod. Phys., Part C2, A177 (2002).

[5] M. Bender, P. H. Heenen, P. G. Reinhard, Rev. Mod. Phys. 75, 121 (2003).

[6] D. Vretenar, A. V. Afanasjev, G. A. Lalazissis, P. Ring, Phys. Rep. **409**, 101 (2005).

[7] Yu. Ts. Oganessian *et al*, Nucl. Phys. **A734**, 109 (2004).

[8] S. Hofmann *et al*, Nucl. Phys. **A734**, 93 (2004).

[9] A. V. Afanasjev, P. Ring, and J. König, Nucl. Phys. **A676**, 196 (2000).

[10] C. Mahaux, P. F. Bortignon, R. A. Broglia, and C. H. Dasso, Phys. Rep. **120**, 1 (1985).

[11] A. Bohr and B. R. Mottelson, *Nuclear Structure*, Vol. II (World Scientific, 1998).

[12] V. G. Soloviev, *Theory of Complex Nuclei* (Pergamon, 1976).

[13] W. Koepf and P. Ring, Nucl. Phys. **A493**, 61 (1989).

[14] A. V. Afanasjev, J. König, and P. Ring, Phys. Rev. C **60**, 051303 (1999).

[15] M. Jaminon and C. Mahaux, Phys. Rev. **C40**, 354 (1989).

[16] M. Bender, K. Rutz, P.-G. Reinhard, J. A. Maruhn, W. Greiner, Phys. Rev. C **60**, 034304 (1999).

[17] G. A. Lalazissis, M. M. Sharma, P. Ring and Y. K. Gambhir, Nucl. Phys. **A608**, 202 (1996).

[18] M. Rashdan, Phys. Rev. C **63**, 044303 (2001).

[19] T. Nikšić, D. Vretenar, P. Finelli, and P. Ring, Phys. Rev. C **66**, 024306 (2002).

[20] G. A. Lalazissis, T. Nikšić, D. Vretenar, P. Ring, Phys. Rev. C **71**, 024312 (2005).

[21] A. V. Afanasjev and S. Frauendorf, Phys. Rev. C **71**, 024308 (2005).

[22] J. Decharge, J.-F. Berger, K. Dietrich, and M. S. Weiss, Phys. Lett. **B451**, 275 (1999).

[23] Y. K. Gambhir, P. Ring and A. Thimet, Ann. Phys. **198**, 132 (1990).

[24] P.-G. Reinhard, M. Rufa, J. Maruhn, W. Greiner and J. Friedrich, Z. Phys. **A323**, 13 (1986).

[25] G. A. Lalazissis, J. König, and P. Ring, Phys. Rev. C **55**, 540 (1997).

[26] S. Hofmann and G. Münzenberg, Rev. Mod. Phys. **72**, 733 (2000).

[27] Yu. Ts. Oganessian, Nucl. Phys. **A685**, 17c (2001).

[28] R. R. Chasman, I. Ahmad, A. M. Friedman, and J. R. Erskine, Rev. Mod. Phys. **49**, 833 (1977).

[29] J. C. Pei, F. R. Xu and P. D. Stevenson, Phys. Rev. C71, 034302 (2005).

[30] P. Möller and J. R. Nix, J. Phys. G20, 1681 (1994).

[31] Z. Patyk and A. Sobiczewski, Nucl. Phys. **A533**, 132 (1991).

[32] T. Sil, S. K. Patra, B. K. Sharma, M. Centelles and X. Vinas, Phys. Rev. C **69**, 044315 (2004).

[33] W. Zhang, J. Meng, S. Q. Zhang, L. S. Geng, H. Toki, Nucl. Phys. **A753**, 106 (2005).

[34] P. Ring and P. Schuck, *The Nuclear Many-Body Problem*, Springer-Verlag, Heidelberg, 1980.

[35] M. Anguiano, J. L. Egido, and L. M. Robledo, Phys. Lett. **B545**, 62 (2002).

[36] M. Farine, J. M. Pearson, F. Tondeur, Nucl. Phys. **A696**, 396 (2001).